Submitted to ApJL
Preprint typeset using LaTeX style emulateapj v. 11/12/01

STAR FORMATION EFFICIENCY IN DRIVEN, SUPERCRITICAL, TURBULENT CLOUDS

Enrique Vázquez-Semadeni[1], Jongsoo Kim[2] and Javier Ballesteros-Paredes[1]
Submitted to ApJL

ABSTRACT

We present measurements of the star formation efficiency (SFE) in 3D numerical simulations of driven turbulence in supercritical, ideal-MHD, and non-magnetic regimes, characterized by their mean normalized mass-to-flux ratio μ, all with 64 Jeans masses and similar rms Mach numbers (~ 10). In most cases, the moderately supercritical runs with $\mu = 2.8$ have significantly lower SFEs than the non-magnetic cases, being comparable to observational estimates for whole molecular clouds ($\lesssim 5\%$ over 4 Myr). Also, as the mean field is increased, the number of collapsed objects decreases, and the median mass of the collapsed objects increases. However, the largest collapsed-object masses systematically occur in the weak-field case $\mu = 8.8$. The high-density tails of the density histograms in the simulations are depressed as the mean magnetic field strength is increased. This suggests that the smaller numbers and larger masses of the collapsed objects in the magnetic cases may be due to a greater scarcity and lower mean densities (implying larger Jeans masses) of the collapse candidates. In this scenario, the effect of a weak field is to reduce the probability of a core reaching its thermal Jeans mass, even if it is supercritical. We thus suggest that the SFE may be monotonically reduced as the field strength increases from zero to subcritical values, rather than there being a discontinuous transition between the sub- and supercritical regimes, and that a crucial question to address is whether the turbulence in molecular clouds is driven or decaying, with current observational and theoretical evidence favoring (albeit inconclusively) the driven regime.

Subject headings: ISM: clouds — MHD — Stars: formation — Turbulence

1. INTRODUCTION

The fraction of a molecular gas mass that is converted into stars, known as the star formation efficiency (SFE), is known to be small, ranging from a few percent for entire molecular cloud complexes (e.g., Myers et al. 1986) to 10–30% for cluster-forming cores (e.g., Lada & Lada 2003), even though molecular clouds in general have masses much larger than their thermal Jeans masses, and should therefore be undergoing generalized gravitational collapse if no other processes prevented it (Zuckerman & Palmer 1974). Thus, this reduction of the mass that is deposited in collapsed objects needs to be accounted for by models of the star formation process.

In the so-called "turbulent" model of star formation (see, e.g., the reviews by Vázquez-Semadeni et al. 2000; Mac Low & Klessen 2004; Vázquez-Semadeni 2004), the low efficiency arises because the supersonic turbulence within the clouds, while contributing to global support, generates large-amplitude density fluctuations (clumps and cores), some of which may themselves become locally gravitationally unstable and collapse in times much shorter than the cloud's global free-fall time. Thus, collapse occurs locally rather than globally, and involves only a fraction of the cloud's total mass. This fraction constitutes the SFE, and depends on the global properties of the cloud, such as its rms Mach number, the number of Jeans masses it contains, and the turbulence driving scale (Léorat, Passot & Pouquet 1990; Klessen, Heitsch & Mac Low 2000), or, perhaps more physically, on the scale at which the turbulent velocity dispersion becomes subsonic (Padoan 1995; Vázquez-Semadeni, Ballesteros-Paredes & Klessen 2003). Nevertheless, the SFE appears to still be too large in non-magnetic configurations, being $\sim 30\%$ in simulations with realistic parameters (e.g., Klessen, Heitsch & Mac Low 2000; Vázquez-Semadeni, Ballesteros-Paredes & Klessen 2003), and it is important to investigate the contribution of the magnetic field in further reducing the SFE. This remains an open issue. In three-dimensional (3D) simulations of driven, self-gravitating, ideal MHD turbulence, Heitsch, Mac Low & Klessen (2001) studied the evolution of the mass fraction in collapsed objects (a measure of the SFE) in supercritical and non-magnetic cases. They reported, however, that any systematic trends with the field strength that might have been present in their simulations were blurred by statistical fluctuations from one realization to another.

More recently, Li & Nakamura (2004, hereafter LN04) and Nakamura & Li (2005, hereafter NL05), have measured the SFE in two-dimensional (2D) simulations of *decaying* turbulence including ambipolar diffusion (AD) and (in NL05) a model prescription for outflows. LN04 found that the initial turbulence can accelerate the formation and collapse of cores within the clouds. NL05 concluded that SFEs comparable to those of whole molecular clouds (a few percent) required moderately subcritical conditions, while moderately supercritical cases gave efficiencies comparable to cluster-forming cores ($\sim 20\%$). However, since their simulations were done in a decaying regime and in a closed numerical box, the SFEs they measured are probably upper limits. Real clouds may not be in a decaying regime (Vázquez-Semadeni et al. 2005, hereafter Paper I;

[1] Centro de Radioastronomía y Astrofísica (CRyA), UNAM, Apdo. Postal 72-3 (Xangari), Morelia, Michoacán 58089, México (e.vazquez, j.ballesteros@astrosmo.unam.mx)
[2] Korea Astronomy and Space Science Institute (KASI), 61-1, Hwaam-Dong, Yusong-Ku, Daejeon, 305-348, Korea (jskim@kasi.re.kr)

see also the discussion in §4) and moreover probably undergo partial dispersion in response to their turbulent energy contents, as in the simulations of Clark & Bonnell (2004) and Clark et al. (2005), thus reducing the amount of mass available for collapse.

Paper I studied the formation, evolution and collapse of the cores formed in 3D simulations of *driven* MHD turbulence, albeit neglecting AD. Due to this setup, no collapse could occur in subcritical cases. Although no quantitative measurements of the SFE were reported there, a trend towards decreasing collapse rates with increasing field strengths was clearly observed in supercritical and non-magnetic cases. This was *not* due to longer individual core collapse times in the magnetic cases with respect to the non-magnetic one, since the timescales for formation and collapse of the cores were similar in both cases. Instead, the reduction of the SFE was apparently due to a reduced formation rate of collapsing objects in the magnetic simulations in comparison with the non-magnetic case.

The goal of the present paper is to report quantitative measurements of the SFE and of the numbers and masses of collapsed objects forming in the simulations of Paper I and three new sets of similar ones, as a function of the mean field strength. In order to overcome the difficulties encountered by Heitsch, Mac Low & Klessen (2001), we study these variables at fixed settings of the random turbulence driver.

2. NUMERICAL METHOD, SIMULATIONS AND PROCEDURE

We refer the reader to Paper I for details on the simulations and resolution considerations. We consider four sets of simulations at a resolution of 256^3 keeping all physical parameters constant, except for the mass-to-magnetic flux ratio μ, which we vary to investigate the effects of the magnetic field. One set consists of the four simulations presented in Paper I with rms Mach number $M \approx 10$, Jeans number $J \equiv L/L_{\rm J} = 4$ (where L is the numerical box size and $L_{\rm J}$ is the Jeans length), and $\mu = 0.9$, 2.8, 8.8 and ∞, corresponding to subcritical, moderately supercritical, strongly supercritical and non-magnetic cases. We refer to this set by the label "Paper I". We also consider three more sets of three similar simulations each (with $\mu = 2.8$, 8.8 and ∞), but varying the seed of the random turbulence driver. We label the sets by their seed numbers, as "Seed = 0.1", "Seed = 0.2", and "Seed = 0.3". The driving is computed in Fourier space, and applied at the largest scales in the simulation ($\sim 1/2$ of the box length), so that it is not expected to be the main driver of the local evolution of the clumps and cores, because, on the scales of the cores, the applied force is nearly uniform, and its main effect should just be to push the cores around without severely distorting them.

Although the simulations are scale-free, for reference, a convenient set of physical units is $n_0 = 500$ cm^{-3}, $u_0 = c_{\rm s} = 0.2$ km s^{-1}, $L_0 = L = 4$ pc, and $t_0 = L_0/u_0 = 20$ Myr. The latter is the sound crossing time across the box. Taking the mean molecular mass as $m = 2.4 m_{\rm H}$, the numerical box then contains $1.86 \times 10^3 {\rm M}_\odot$. The mean field strengths for the $\mu = 0.9$, 2.8, 8.8 and ∞ cases are respectively $B_0 = 45.8$, 14.5, 4.58, and 0 μG, corresponding to values of β, the ratio of thermal to magnetic pressure, of $\beta = 0.01$, 0.1, 1 and ∞. The simulations are run for 0.5 code time units (10 Myr) before turning on the self-gravity.

As a measure of the SFE, we consider the evolution of the collapsed mass fraction $M_{\rm col}$ of the simulations. By this we mean gas that is at densities $n > 500 n_0$, since in Paper I we noticed that once an object reached densities $\sim 300 n_0$ it was always already on its way to collapse, a fact which is confirmed by the fact that these objects never disperse during the subsequent evolution of the simulations. Throughout the paper, we refer exclusively to collapsed objects rather than stars, because our spatial resolution is clearly insufficient to determine whether a collapsing object eventually breaks up into more fragments to form several stars. This is likely to be the case for the most massive collapsed objects, with masses up to ~ 100 M$_\odot$. Thus, the masses reported in fig. 2 should not be necessarily interpreted as individual stellar masses, and may well be cluster masses. Also note that in runs that form a single collapsed object, the plots of $M_{\rm col}$ vs. time really represent the accretion history onto that object, rather than the continuous formation of new collapsed objects.

As a representative cloud lifetime we take $\tau_{\rm cl} = 4$ Myr, a time scale that agrees with the estimate of Bergin et al. (2004) of 3–5 Myr and also with the two-turbulent-crossing-times criterion used by Vázquez-Semadeni, Ballesteros-Paredes & Klessen (2003). Quoted values of the SFE refer to the collapsed mass fraction at $t = \tau_{\rm cl}$. Note, however, that, because of numerical problems when the density contrast becomes too large, not all simulations reach this time, although this will not be a limitation for the conclusions we will draw.

3. RESULTS

Figure 1 shows the evolution of the accreted mass fraction for the four sets of runs we consider. The moderately supercritical runs, with $\mu = 2.8$, have generally lower SFEs than both the strongly supercritical ($\mu = 8.8$) and non-magnetic ($\mu = \infty$) runs. In turn, the $\mu = 8.8$ cases have SFEs that are generally very similar to those of the non-magnetic runs, except in the runs from Paper I. It is also noteworthy that the $\mu = 2.8$ cases have SFEs ≈ 0.04, 0.12, 0.025 and 0.05, respectively for each set. Thus, in three out of the four statistical realizations, $M_{\rm col} \leq 5\%$ at $t = \tau_{\rm cl}$, in reasonable agreement with the observed SFEs at the level of global molecular clouds.

What is even more interesting is the different way in which the magnetic and the non-magnetic runs reach their respective collapsed fractions. Figures 5 and 9 in Paper I, and their corresponding animations in the electronic version, show that, while the magnetic runs do so with one or two relatively massive collapsed objects, the non-magnetic run does so with several objects, many of them with low masses. The same trend is observed in the three additional sets of statistical realizations considered in the present paper. In fig. 2 we show the masses of the individual collapsed objects ($n > 500 n_0$) for all the runs we consider at $t = 4$ Myr, except for those cases in which the simulation terminated prematurely, in which case we plot the collapsed object masses at the last timestep of the simulation. We see that the non-magnetic runs typically produce many more collapsed objects than the magnetic runs, and with mass distributions that extend to significantly lower values. On half the cases, the minimum masses of the col-

lapsed objects increase monotonically with increasing field strength.

One of the main results of Paper I was that the core formation+collapse time scale was not significantly different between the magnetic and non-magnetic cases. Thus, the above result on the masses and numbers of the collapsed objects suggest that the decreased efficiency of the magnetic cases in comparison to the non-magnetic ones arises from a decreased probability of collapse events as the field strength increases, rather than from an increase of the collapsing object lifetimes. This suggestion is supported by the probability distribution of the density fluctuations for the various runs. Figure 3 shows the histograms of the density values in each of the simulations, averaged over the last five snapshots before turning on gravity. In this figure, the panel for the runs from Paper I includes the subcritical run with $\mu = 0.9$, in order to see the effect of the magnetic field in this case as well, even though this run did not undergo collapse.

Figure 3 shows a clear trend towards decreasing width and lower high-density tails with increasing mean field strength (increasing μ), at least over the range of magnetic field strengths we have considered here. That is, the probability of producing large density enhancements decreases with increasing magnetic field strength. This is in agreement with previous results by Passot, Vázquez-Semadeni & Pouquet (1995), Ostriker, Gammie & Stone (1999), Heitsch, Mac Low & Klessen (2001) and Ballesteros-Paredes & Mac Low (2002). Note, however, that in those works a reverse trend towards increasing fluctuation amplitude was observed at stronger values of the field, which we do not observe here, again at least over the field strength range spanned by our simulations.

The trend towards lower and less extended high-density tails in the histograms at larger field strengths is consistent with the trend of the SFE to decrease and of the minimum collapsed masses to increase in the same limit, since fewer density fluctuations can reach the threshold for collapse, and simultaneously, the local values of the Jeans mass are larger, so that, in order to collapse, an object needs to acquire more mass. In this picture, the field's effect on the SFE is only indirect, through its modification of the density histogram, rather than by directly increasing the minimum mass for collapse (i.e., by causing the magnetically critical mass of the cores to be larger than their Jeans masses). Indeed, in the cases studied in Paper I, examples of both collapsing and non-collapsing cores were supercritical, and the occurrence of collapse depended on whether they acquired the Jeans mass. Similarly, Li et al. (2004) found that all the cores in their supercritical simulations were supercritical.

Finally, it is worth noting that the most massive objects systematically arise in the strongly supercritical cases ($\mu = 8.8$) in all four simulation sets. The origin of this effect, as well as a test of the mechanism suggested above for reducing the SFE and increasing the minimum masses will require detailed measurements of the field morphology and the evolution of the energy balance in the cores prior and during the onset of collapse, to be presented elsewhere.

4. DISCUSSION

The above results can be placed in the context of previous studies. We have found that the presence of a magnetic field can further reduce the SFE with respect to the non-magnetic case, even in supercritical configurations. Previous successful determinations of the effect of the magnetic field have been restricted to decaying, 2D simulations (LN04; NL05). These authors found that values of the SFE comparable to those observed in entire molecular clouds (a few percent; Myers et al. 1986) required subcritical environments and AD-mediated collapse, while supercritical environments gave values of the SFE closer to those of cluster-forming cores ($\sim 15\%$ after 1 global free-fall time).

Instead, in our simulations we have found that a moderately supercritical environment and reasonably realistic values of the Mach number (10) and of the Jeans number (64 Jeans masses in a 4-pc cube) already give SFEs $\lesssim 5\%$ in 3/4 of the cases studied after 0.8 global free-fall times (4 Myr), in spite of having a mass-to-flux ratio more than twice larger than theirs. The difference is probably due mainly to the choice of global setup (2D, decaying, versus 3D, driven), since a continuously-driven simulation maintains the turbulent support throughout its evolution, while a decaying one loses it over time.

In the simulations of LN04 and NL05, the main role of turbulence is to accelerate the initial formation of the cores and other density structures, which occurs on the turbulent crossing time rather than in the long AD timescale. However, as the turbulence decays, its role in providing support and producing further fragmentation (which induces *local* collapse involving small fractions of the total mass) progressively decreases. Indeed, the turbulent Mach numbers in the simulations of NL05 had already decayed to values $\sim$ 2–3 by the times the collapsed objects were forming. Thus, in their supercritical cases, the entire bulk mass of the simulation is in principle available for collapse at long enough times, although the residual turbulent fragmentation still drives local collapse events first.

This suggests that a fundamental question in understanding the SFE in molecular clouds is whether real molecular clouds are driven or decaying, and sub- or supercritical. Concerning the former dichotomy, observational evidence tends to suggest that molecular clouds are driven, as we discussed at length in Paper I; a few additional considerations are as follows. If the turbulence is generated by instabilities in the compressed layers as the clouds are forming (e.g., Hunter et al. 1986; Vishniac 1994; Walder & Folini 2000), the injection of turbulent energy is likely to last for as long as the accumulation process lasts. Afterwards, the cloud is likely to disperse, as indicated by the facts that the gas has disappeared from star-forming regions after a few Myr (Hartmann, Ballesteros-Paredes & Bergin 2001), and that all clouds of comparable masses tend to have comparable levels of turbulence (Heyer & Brunt 2004). If the turbulence in clouds were decaying, one would expect that clouds of a given mass would exhibit a large scatter in their turbulence levels, contrary to what is observed. The "universal" behavior of the turbulent level in clouds reported by Heyer & Brunt (2004) also suggests that the clouds are part of the global Galactic turbulent cascade, in which the key process is a *statistically stationary* energy transfer among scales, analo-

gous to the classical Kolmogorv cascade. Thus, driven-turbulence simulations may be a somewhat better approximation to real clouds than decaying ones, although the standard Fourier-driving scheme is likely not to be the best model of the true injection mechanism. Simulations with more realistic driving schemes are clearly needed.

Concerning the subcritical vs. supercritical dichotomy, theoretical arguments suggest that as a cloud is becoming predominantly molecular and self-gravitating, it is also becoming supercritical (McKee 1989; Hartmann, Ballesteros-Paredes & Bergin 2001). Recent observational evidence remains inconclusive, and tends to suggest that both kinds are realized, with probably some preponderance of supercritical ones (Crutcher 1999; Bourke et al. 2001; Crutcher 2004), although the uncertainties are large. The safest assumption at this point appears to be that both regimes are realized in molecular clouds.

Thus, the global picture that emerges is that a *distribution* of magnetic field strengths exists in the ensemble of molecular clouds (Ballesteros-Paredes & Vázquez-Semadeni 1997), and that the SFE decreases monotonically as the mean field strength in the clouds is larger. This appears to be a *continuous* trend, rather than a sharp dichotomy between sub- and supercritical regimes, as was the case in the standard model of star formation (Shu, Adams & Lizano 1987; Mouschovias 1991). The role of AD would then mostly be to just allow subcritical clouds to participate in the star formation process, with the lowest SFEs of the spectrum. A confirmation of this picture will require a systematic study of the SFE in 3D, driven simulations including AD, to be presented elsewhere.

Our second result is that the number of collapsed objects appears to decrease, and their median mass appears to increase with increasing mean field strength. This result is consistent with the observation that in the non-magnetic case a single clump appears to form several collapsed objects, while in the magnetic cases a clump appears to form a single object, as can be seen in the animations presented in Paper I. This observation goes in line with the findings of Heitsch, Mac Low & Klessen (2001), who noticed that non-magnetic simulations with large-scale driving tended to form *clusters* of collapsed objects, while magnetic cases tended to form the collapsed objects in a more scattered fashion. If collapsing objects in the magnetic case are more massive, then clumps of a given mass can form fewer objects. Detailed analysis of the evolution of individual cores will be necessary to test these possibilities.

This work has received partial financial support from grants CONACYT 36571-E to E.V.-S. J.K. was supported by ARCSEC, of the Korea Science and Engineering Foundation, through the SRC program. The numerical simulations have been performed on the linux clusters at KASI (funded by KASI and ARCSEC) and at CRyA (funded by the above CONACYT grant).

REFERENCES

Ballesteros-Paredes, J., & Vázquez-Semadeni, E. 1997, in "Star Formation, Near and Far. 7th Annual Astrophysics Conference in Maryland", ed. S. Holt and L. Mundy (New York: AIP Press), p.81
Ballesteros-Paredes, J. & Mac Low, M. 2002, ApJ, 570, 734
Bergin, E. A., Hartmann, L. W., Raymond, J. C., Ballesteros-Paredes, J. 2004, ApJ 612, 921
Bourke, T. L., Myers, P. C., Robinson, G., Hyland, A. R. 2001, ApJ 554, 916
Clark, P. C. & Bonnell, I. A. 2004, MNRAS 347, L36
Clark, P. C., Bonnell, I. A., Zinnecker, H., & Bate, M. A. 2005, MNRAS, in press (astro-ph/0503141)
Crutcher, R. M. 1999, ApJ 520, 706
Crutcher, R. 2004, ApSS 292, 225; prceedings of "Magnetic Fields and Star Formation: Theory versus Observations", eds. Ana I. Gomez de Castro et al.
Hartmann, L., Ballesteros-Paredes, J., & Bergin, E. A. 2001, ApJ, 562, 852
Hartmann, L. 2003, ApJ 585, 398
Heitsch, F., Mac Low, M. M., & Klessen, R. S. 2001, ApJ, 547, 280
Heyer, M. H. & Brunt, C. M. 2004, ApJ 615, L45
Hunter, J. H., Jr., Sandford, M. T., II, Whitaker, R. W., Klein, R. I. 1986, ApJ 305, 309
Klessen, R. S., Heitsch, F., & MacLow, M. M. 2000, ApJ, 535, 887
Lada, C. J. & Lada, E. A. 2003, ARAA 41, 57
Léorat, J., Passot, T. & Pouquet, A. 1990, MNRAS 243, 293
Li, Z.-Y. & Nakamura, F. 2004, ApJ 609, L83 (LN04)
Li, P. S., Norman, M. L., Mac Low, M.-M. & Heitsch, F. 2004, ApJ 605, 800
Mac Low, M.-M. & Klessen, R. S. 2004, Rev. Mod. Phys. 76, 125
McKee, C. F. 1989, ApJ 345, 782
Mouschovias, T. Ch. 1991, in "The Physics of Star Formation and Early Stellar Evolution", eds. C. F. Lada and N. Kylafis (Dordrech: Kluwer), 449
Myers, P. C., Dame, T. M., Thaddeus, P., Cohen, R. S., Silverberg, R. F., Dwek, E. & Hauser, M. G. 1986, ApJ 301, 398
Nakamura, F. & Li, Z.-Y. 2005, ApJ, submitted (NL05; astro-ph/0502130)
Ostriker, E. C., Gammie, C. F. & Stone, J. M. 1999, ApJ 513, 259
Padoan, P. 1995, MNRAS, 277, 377
Passot, T., Vázquez-Semadeni, E. & Pouquet, A. 1995, ApJ 455, 536
Shu, F. H., Adams, F. C., & Lizano, S. 1987, ARAA, 25, 23
Vázquez-Semadeni, E., Ostriker, E. C., Passot, T., Gammie, C. & Stone, J., 2000, in "Protostars & Planets IV", ed. V. Mannings, A. Boss & S. Russell (Tucson: Univ. of Arizona Press), 3
Vázquez-Semadeni, E., Ballesteros-Paredes, J. & Klessen, R. S. 2003, ApJ 585, L131
Vázquez-Semadeni, E. 2004, in "IMF@50: the Initial Mass Function 50 Years Later", eds. E. Corbelli, F. Palla, and H. Zinnecker, in press (astro-ph/0409553)
Vázquez-Semadeni, E., Kim, J., Shadmehri, M. Ballesteros-Paredes, J. 2005, ApJ 618, 344 (Paper I)
Vishniac, E. T. 1994, ApJ 428, 186
Walder, R. & Folini, D. 2000, ApSS 274, 343
Zuckerman, B. & Palmer, P. 1974, ARAA 12, 279

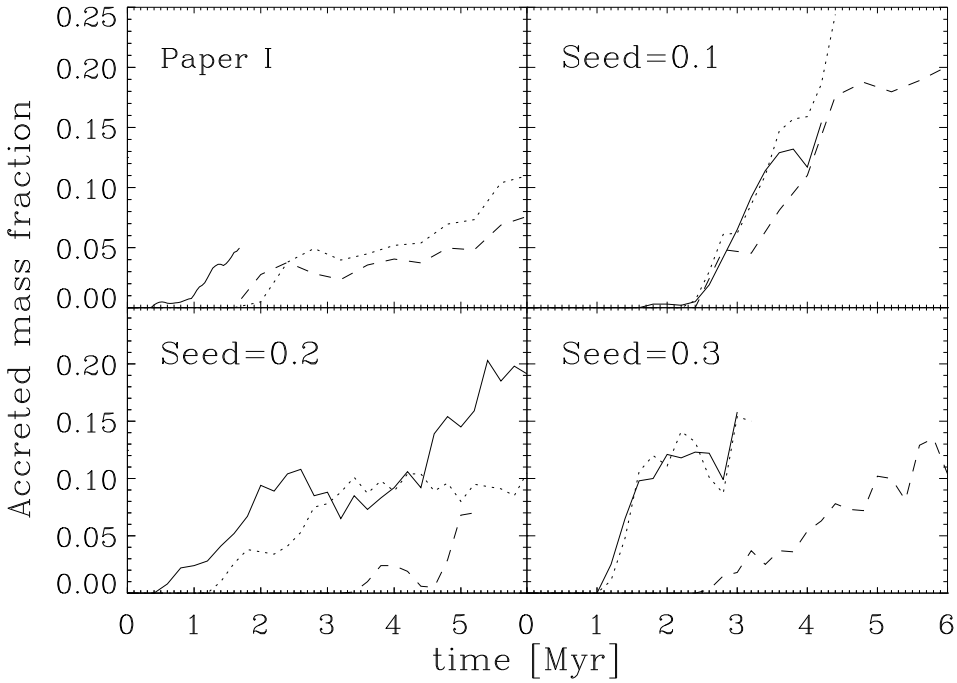

FIG. 1.— Evolution of the accreted mass fraction for the four sets of runs considered. *Solid* lines denote $\mu = \infty$, *dotted* lines denote $\mu = 8.8$, and *dashed lines* denote $\mu = 2.8$.

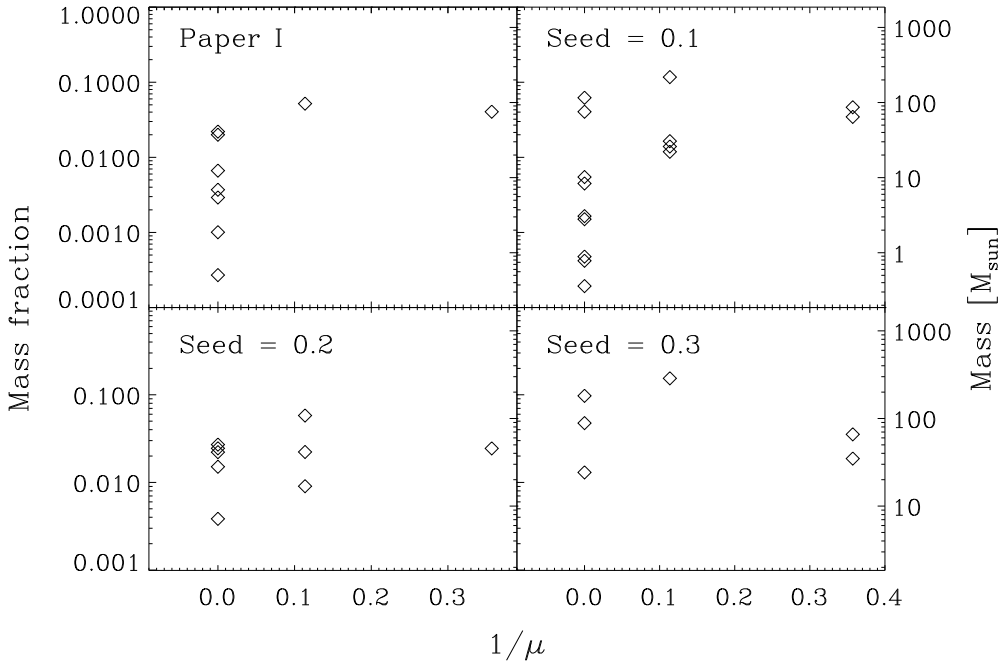

FIG. 2.— Masses of the collapsed objects (objects with densities $n > 500n_0$) versus the inverse of the simulation mass-to-flux ratio for the four sets of runs. The left vertical axis gives the masses as fractions of the total mass in the simulation, and the right axis gives them in solar masses, according to the adopted normalization.

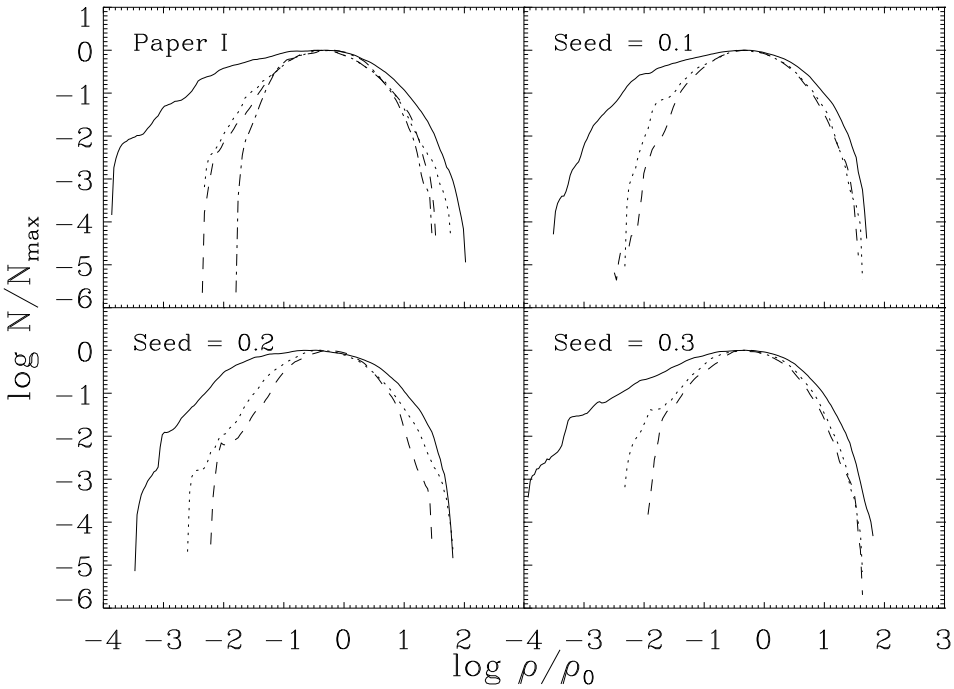

FIG. 3.— Normalized density histograms for all the simulations immediately before gravity is turned on. The line coding is as in fig. 1. The *dot-dashed* line in the "Paper I" panel denotes the subcritical case with $\mu = 0.9$.